Critical temperature and specific heat for Cooper pairing on a spherical surface

V. N. Gladilin,[1,*] J. Tempere,[1,2] I. F. Silvera,[2] and J. T. Devreese[1]
[1]*TFVS, Universiteit Antwerpen, Universiteitsplein 1, B-2610 Antwerpen, Belgium*
[2]*Lyman Laboratory of Physics, Harvard University, Cambridge, Massachusetts 02138, USA*
(Received 20 March 2006; revised manuscript received 28 July 2006; published 28 September 2006)

Based on an exact solution of the Bardeen-Cooper-Schrieffer-type Hamiltonian on a spherical surface, we calculate the specific heat for the electron system with pair correlations on a sphere. We find that it is possible to extract from the specific heat a temperature above which many-body states with broken Cooper pairs get populated. Therefore, we define this temperature as the characteristic temperature signaling the onset of a BCS-type pair-correlated state for electrons on a spherical surface. Such spherical electron systems are realized in multielectron bubbles in liquid helium, for which the above-mentioned characteristic temperature is found to be of the order of 10–100 mK. Both the specific heat and the critical temperature show a pronounced (4–6 %) odd-even parity effect that persists even for numbers of electrons as large as 10^6.

DOI: 10.1103/PhysRevB.74.104512 PACS number(s): 74.20.Fg, 71.10.Pm, 74.78.−w, 74.10.+v

I. INTRODUCTION

The physics of the two-dimensional electron system remains the subject of intense theoretical and experimental scrutiny. Spherical two-dimensional electron systems have not been as thoroughly investigated as their flat counterparts, despite the fact that the spherical geometry is expected to lead to new physics because of its intrinsic topological difference with a flat space.[1] Moreover, the presence of curvature also influences the coupling of the system to magnetic fields, as has been shown for spherical[2] and toroidal electron systems.[3]

Spherical two-dimensional electron systems appear in various physical systems: prominent examples are metallic nanoshells[4] and buckyballs.[5] The most idealized realization of a spherical two-dimensional electron system is found in a multielectron bubble (MEB) in liquid helium. MEBs are (typically micron-sized) cavities in the liquid, containing anywhere from a few up to 10^8 electrons. They have first been observed as a result of a surface instability that occurs when a liquid helium surface is being charged with electrons beyond a critical surface charge density.[6]

The bare single electron states on the surface of a spherical bubble are angular momentum eigenstates and have discrete energies, characterized by the angular momentum L and with degeneracy $2L+1$. At low temperature there will be a well-defined Fermi surface located at the highest occupied state. Small-amplitude shape oscillations, including surface waves, can be quantized as spherical ripplons, described by the Hamiltonian

$$\hat{H}_{\mathrm{ripl}} = \sum_{L>0,m} \hbar\omega_L \hat{a}^+_{L,m}\hat{a}_{L,m}, \tag{1}$$

where $\hat{a}^+_{L,m}$ ($\hat{a}_{L,m}$) is the creation (annihilation) operator for a ripplon with angular momentum L and its z-projection m. ω_L are the ripplonic frequencies derived in Ref. 7 for spherical MEBs under external pressure. The electrons can interact with these ripplons. The interaction between electrons and ripplons on the bubble surface is analogous to that of electrons and phonons in solids. In particular, it can lead to the formation of ripplonic polarons.[8] In a recent work, the present authors have shown that the electron-ripplon interaction leads to the formation of strong pairing correlations below a critical temperature.[9] These pairing correlations are similar to the Bardeen-Cooper-Schrieffer (BCS) superconducting pair correlations in metals. This raises the obvious question of how "superconductivity" will manifest itself on a micron-sized spherical surface. More specifically, one can ask how the formation of strong pairing correlations can be detected experimentally, and how the critical temperature can be determined.

In their study of nanoscopic superconducting aluminum particles, Black *et al.*[10] used electron tunneling spectroscopy to detect the superconducting excitation gap. Also in multielectron bubbles, pairing correlations lead to a (pseudo)gap in the density of states.[9] In the present paper, we investigate observable manifestations of pairing correlations in MEBs. The altered density of states will reflect itself in particular in the specific heat of the system. Below, we calculate the specific heat of the spherical two-dimensional electron system and argue that the onset of a sharp rise in the specific heat can be used to define a characteristic temperature for the transition between a normal state and the pair-correlated state. Moreover, we derive an analytical expression for this characteristic temperature and show that the specific heat reveals a pronounced odd-even parity effect, which persists even for large (10^6) numbers of electrons.

II. SPECIFIC HEAT OF COOPER PAIRS ON A SPHERE

The spherical, two-dimensional electron system, is described in second quantization with the operators $\hat{c}^+_{\ell,m,\sigma}$ and $\hat{c}_{\ell,m,\sigma}$ that create, respectively, destroy an electron with spin $\sigma=\uparrow,\downarrow$ in the angular momentum eigenstate $|\ell,m\rangle$. In Ref. 9 we have shown that in the case of multielectron bubbles, the electron-ripplon interaction leads to a Cooper-type attractive interaction between the electrons, resulting in a BCS-type Hamiltonian:

 ©2006 The American Physical Society

$$\hat{H} = \sum_{\ell=0}^{\infty} \left(\sum_{m=-\ell}^{\ell} \sum_{\sigma} \epsilon_\ell \hat{c}^+_{\ell,m,\sigma} \hat{c}_{\ell,m,\sigma} - G \sum_{m,m'=-\ell}^{\ell} \hat{c}^+_{\ell,-m',\downarrow} \hat{c}^+_{\ell,m',\uparrow} \hat{c}_{\ell,m,\uparrow} \hat{c}_{\ell,-m,\downarrow} \right). \quad (2)$$

This Hamiltonian can be mapped onto the so-called "reduced BCS Hamiltonian" studied in the context of superconducting nanograins.[11,12] In the present case, ϵ_ℓ represents the unperturbed, $2(2\ell+1)$-degenerate angular-momentum energy level

$$\epsilon_\ell = \frac{\hbar^2}{2m_e R^2} \ell(\ell+1), \quad (3)$$

where m_e is the electron mass and R is the radius of the spherical system. The separation between different angular momentum levels ℓ of the unperturbed system is typically much larger than the energy of the ripplons, and the interacting electron-ripplon system can effectively be treated as a sum over subsystems with different ℓ. The typical energy scale of the kinetic energy is $\epsilon_1 = \hbar^2/(m_e R^2)$. For a 10 000 electron bubble at zero external pressure, $\epsilon_1 = 0.78$ mK. The interaction energy scale G for the same bubble lies around $G = 10$ mK, and the ripplon energy scale for this bubble is 10 μK. In what follows, we will present results as a function of the dimensionless coupling constant G/ϵ_1.

The Hamiltonian (2) can be solved analytically, using Richardson's method.[13,14] The total energy is a sum of the energies for each ℓ subsystem,

$$E_j = \sum_{\ell=0}^{\infty} E^{(\ell)}_{n_\ell, g_\ell, b_\ell}, \quad (4)$$

and is characterized by the set of quantum numbers $j = \{n_\ell, g_\ell, b_\ell\}_{\ell=0,1,2,\ldots}$. The energy levels of the subsystem ℓ are given by

$$E^{(\ell)}_{n_\ell, g_\ell, b_\ell} = (2n_\ell + b_\ell)\epsilon_\ell - G(n_\ell - g_\ell)(2\ell - b_\ell + 2 - n_\ell - g_\ell). \quad (5)$$

The quantum number n_ℓ corresponds to the number of electron pairs in the subsystem, whereas b_ℓ is the number of unpaired electrons and g_ℓ is the number of elementary bosonic pair-hole excitations[15] in the system of n_ℓ pairs. In the ground state all electrons are paired ($b_\ell = 0$), except one when an odd number of electrons is present in the system. There are no pair-hole excitations ($g_\ell = 0$) in the ground state. The spherical symmetry, resulting in a discrete and degenerate single-particle level structure, allows for an exact solution of the Hamiltonian (2), describing also the fluctuations.[16] At finite temperatures, two types of excitations will be present. The broken pair states ($b_\ell \neq 0$) correspond on a mean-field level to quasiparticle states in the BCS approximation. The presence of collective modes (in the context of the Richardson solution sometimes called "gaudinos") correspond to the case when $g_\ell \neq 0$.[17]

At strong coupling ($G \geq \epsilon_1/2$) the electron pairs redistribute themselves over approximately $\mu = 2G/\epsilon_1$ different ℓ subsystems around the Fermi level $\ell = L_F$ to minimize the energy.[9] The above estimate for the number of partially occupied angular momentum levels ℓ does not hold for $G \gtrsim N\epsilon_1/2$, where N is the total number of electrons in the system. As implied from Eq. (25) of Ref. 9, at $G \gtrsim N\epsilon_1/2$, when the interaction strength G exceeds the Fermi energy for noninteracting electrons, the ground state would correspond to an electron configuration with just a single pair per ℓ level. However, such an extreme strong-coupling limit appears irrelevant for the multielectron bubbles under consideration and it is not addressed in the following, where the inequality $G \ll N\epsilon_1/2$ is assumed to be satisfied.

The degeneracy of energy level E_j is a product of the degeneracies of the energy levels of the constituent subsystems,

$$J_j = \prod_{\ell=0}^{\infty} J^{(\ell)}_{n_\ell, g_\ell, b_\ell}, \quad (6)$$

with

$$J^{(\ell)}_{n_\ell, g_\ell, b_\ell} = 2^{b_\ell} C^{2\ell+1}_{b_\ell} \begin{cases} 1, & g_\ell = 0, \\ (C^{2\ell+1-b_\ell}_{g_\ell} - C^{2\ell+1-b_\ell}_{g_\ell - 1}), & g_\ell \geq 1, \end{cases} \quad (7)$$

where C^k_n are binomial coefficients.[18]

The analytic expression for the energy levels and their degeneracies allow to compute the specific heat straightforwardly,

$$C = \frac{d\langle E \rangle}{dT}, \quad (8)$$

where $\langle E \rangle$ is the statistical average energy of the electrons in the MEB,

$$\langle E \rangle = \frac{\sum_j J_j E_j \exp[-E_j/(k_B T)]}{\sum_j J_j \exp[-E_j/(k_B T)]}. \quad (9)$$

The density of states $D_\delta(E)$ allows to express this as an energy integral. The subscript δ is used to indicate that we numerically calculate the density of states by counting the states in an energy interval δ around the energy E. For the results presented in Fig. 1, we chose energy intervals of $\delta = 0.01\epsilon_1$. Figure 1 shows the density of states $D_\delta(E)$ as a function of the energy above the ground state energy E_{gs}, for different values of the coupling constant G/ϵ_1. Each graph shows results for both an even (full circles) and an odd (crosses) number N_F of electrons on the highest angular momentum level L_F occupied at $G = 0$. As the coupling constant is increased, a clear odd-even effect appears in the density of states. The presence of an unpaired electron sensitively raises the degeneracy of the energy levels and thus the number of available states.

The aim of the next section is to examine the effect of pairing interactions, described by the Hamiltonian (2) and characterized by the coupling strength G, on the behavior of the specific heat as a function of temperature.

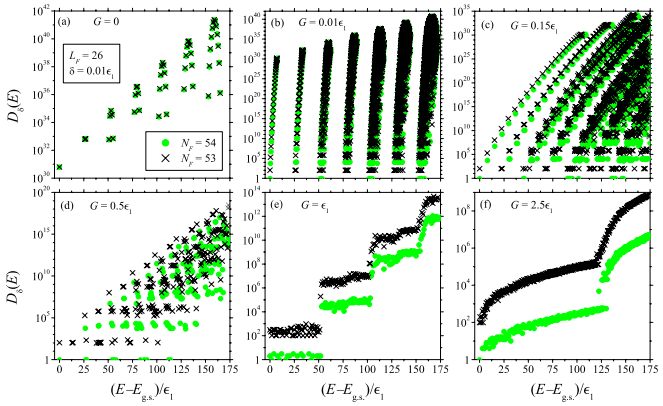

FIG. 1. (Color online) The calculated density of states for a spherical 2D electron system with pairing correlations is shown as a function of the energy above the ground state energy $E_{\rm gs}$. Here $D_\delta(E)$ is evaluated by counting the number of states in an interval $\delta=0.01\epsilon_1$ around energy E. Results are shown for even ($N_F=54$, solid circles) and odd ($N_F=53$, crosses) numbers of electrons on the (unperturbed) Fermi angular momentum level $L_F=26$. The different panels correspond to different strengths of the attractive electron-electron term in the BCS-type Hamiltonian (2).

III. RESULTS AND DISCUSSION

A. Small coupling, $G/\epsilon_1<1/2$

When there are no pairing interactions ($G=0$), the energy level spectrum consists of the discrete levels ϵ_ℓ and the specific heat will be similar to that of a collection of fermionic quantum rotors. It will be small for temperatures $T \ll \hbar^2/(2mR^2k_B)$ and rise rather abruptly to saturate at Nk_B for $T \gg \hbar^2/(2mR^2k_B)$. The onset of the increase of the specific heat at $G=0$ is shown in the full curve in Fig. 2. The increase in the specific heat starts at a temperature where there appears a non-negligible occupation probability for the lowest excited states. These excited states are separated from the ground state by an energy $\sim\epsilon_1(L_F+1)$ and correspond to transitions of electrons between different ℓ subsystems. These transitions will be referred to as *interlevel* transitions.

For small, nonzero $G \ll \epsilon_1$, an additional peak in $C(T)$ develops as shown in Fig. 2. This additional peak appears at a temperature smaller than the temperature at which the $G=0$ specific heat starts to increase. This peak corresponds to *intralevel* excitations of the system: pair breaking and pair-hole excitations. As follows from Eq. (5), the first pair-breaking energy equals the lowest pair-hole excitation energy. For a subsystem ℓ with an even number of electrons, we find $\Delta_\ell=(2\ell+1)G$. For an odd number of electrons, this becomes $\Delta_\ell=2\ell G$.

So, when $G \ll \epsilon_1$, the intralevel excitations occur at energies much smaller than the interlevel excitations. As G is increased, the specific heat peak that corresponds to these intralevel excitations shifts to higher temperatures. In the case of a closed-shell configuration, no intralevel excitations from the ground state are possible, so that no additional peak of $C(T)$ appears at $G \ll \epsilon_1$.

B. Large coupling, $G/\epsilon_1>1/2$

For $G>\epsilon_1/2$, the pair-breaking energy becomes larger than the energy spacing between the single-electron ℓ levels.

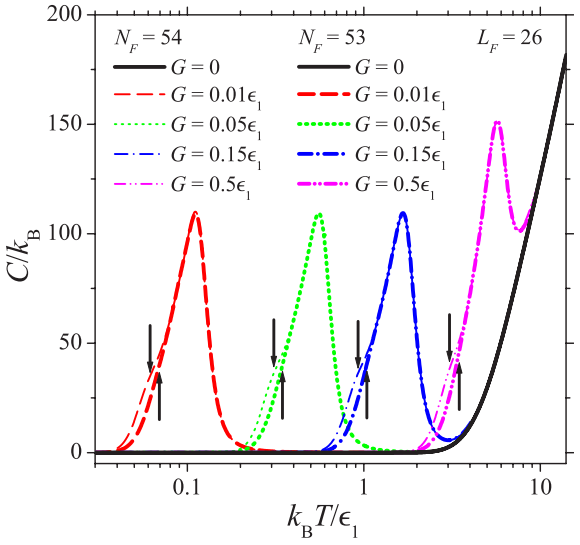

FIG. 2. (Color online) The calculated specific heat is plotted as a function of temperature for an even and odd number of electrons. The results are shown for several values of the interaction strength $G \leqslant \epsilon_1/2$. The down and up arrows are positioned at the corresponding characteristic temperatures given by (11) and (12) for even and odd MEBs, respectively.

The density of states no longer resembles a set of peaks, but it becomes more similar to a step function, where the steps occur at the pair-breaking energy. When the temperature is small enough so as not to populate states with a broken pair, the available density of states is small. But when the temperature is increased and broken pair states become populated, the relevant density of states jumps to a value that is orders of magnitude higher [cf. Figs. 1(e) and 1(f)]. This reflects itself in the behavior of the specific heat: as soon as the temperature is large enough to break pairs, the specific heat will be strongly enhanced. This abrupt transition can be seen in Fig. 3.

The values of the temperature that correspond to the fast increase in $C(T)$ clearly correlate with G. Note that—as distinct from the case of $G/\epsilon_1<1/2$—at large coupling ($G/\epsilon_1>1/2$) the specific heat is nonzero even at temperatures below the temperature of the onset of the rise in C. This is due to the presence of excitations related to interlevel transitions of *pairs*: for large G, these can have energies smaller than the pair-breaking energy. With increasing G, the number of these excitations increases [cf. Fig. 1(f) to Fig. 1(e)], resulting in the corresponding increase of C with G in the low-temperature region (see Fig. 3).

C. The critical temperature for pair breaking

As implied form the previous discussion and from Figs. 2 and 3, both for the case of small ($G<\epsilon_1/2$) and large ($G \geqslant \epsilon_1/2$) coupling the specific heat starts rising at a temperature when states with broken pairs get populated. Below this temperature, BCS-type pairing correlations are dominant, but above this temperature, the "superconducting" pairing correlations are suppressed. So, it is possible to extract from $C(T)$

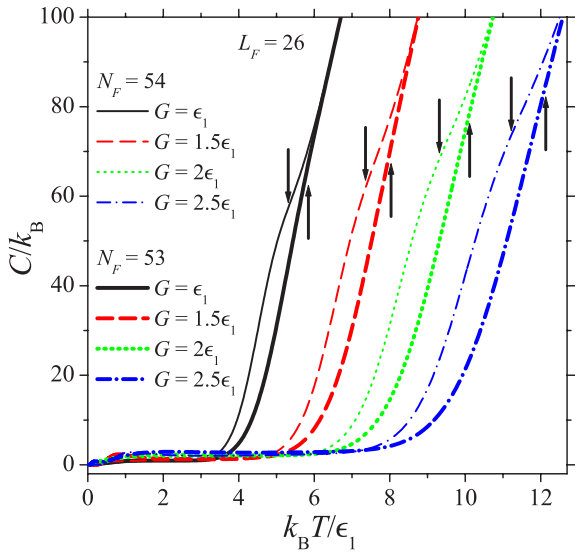

FIG. 3. (Color online) The calculated specific heat is plotted as a function of temperature for an even and odd number of electrons. The results are shown for several values of the interaction strength $G > \varepsilon_1/2$. The down and up arrows are positioned at the corresponding characteristic temperatures given by (11) and (12) for even and odd MEBs, respectively.

a typical temperature T^* separating the two aforementioned regimes.

Here we make an analytical estimate for T^*. The probability for the system to be in the ground state is proportional to $P_{\rm gs}=J_{\rm gs}\exp(-E_{\rm gs}/k_BT)$, where $J_{\rm gs}$ is the degeneracy of the ground state. The probability for the system to break up one pair is proportional to $P_{\rm 1bp}=J_{\rm 1bp}\exp[-(E_{\rm gs}+\Delta_{L_F})/k_BT]$, since Δ_{L_F} is the first pair-breaking energy. Here, $J_{\rm 1bp}$ is the total number of states with one broken pair. An appreciable contribution of states with one broken pair to the specific heat appears when $P_{\rm 1bp}$ becomes comparable to $P_{\rm gs}$, i.e., at a temperature

$$k_BT^* = \frac{\Delta_{L_F}}{\ln(J_{\rm 1bp}/J_{\rm gs})}. \tag{10}$$

The ground state for an even bubble is characterized by $g_\ell=0$, $b_\ell=0$. A state with one broken pair is characterized by $n_\ell \to n_\ell - 1$ and $b_\ell \to b_\ell + 2$. At small coupling, the first pair-breaking takes place for $\ell = L_F$. At strong coupling ($\epsilon_1/2 < G \ll N\epsilon_1/2$), the electron pairs partially occupy about $\mu = 2G/\epsilon_1$ single-particle ℓ levels around the Fermi level L_F and the first pair-breaking can take place on any of these levels (so we still have $\ell \approx L_F$ for $L_F \gg 1$).

From (7) we see that the degeneracy of states that correspond to the first intralevel pair-breaking exceeds that of the ground state by a factor $J_{\rm 1bp}/J_{\rm gs}=4C_2^{2L_F+1}$ ($\approx 8L_F^2$ for $L_F \gg 1$). The ground state for an odd bubble is characterized by $g_\ell=0$, $b_\ell=1$ for the lowest partially occupied subsystem with $\ell \approx L_F$, so that the odd bubble has a ground state that is a factor $2C_1^{2L_F+1}$ more degenerate than that of the even bubble. Applying again Eq. (7) we get for odd bubbles $J_{\rm 1bp}/J_{\rm gs} = 2C_3^{2L_F+1}/C_1^{2L_F+1} \approx 8L_F^2/3$.

Given that the pair-breaking energy is equal to the pair-hole excitation energy, why did we assume that the increase in the specific heat is due to the breaking of pairs rather than to pair-hole excitations? This is justified because the increase in degeneracy due to the pair-breaking is much larger than the increase in degeneracy due to a pair-hole excitation. A pair-hole excitation is characterized by $g_\ell \to g_\ell + 1$ (whereas b_ℓ and n_ℓ are unchanged). From (7) we see that indeed the increase in the degeneracy of states due to the lowest pair-hole excitation (for an even bubble) is characterized by the factor $(C_1^{2L_F+1}-1)$, much smaller than $J_{\rm 1bp}/J_{\rm gs}$ for $L_F \gg 1$.

Thus far, we have only considered intralevel pair breaking. But for $G > \epsilon_1/2$, also interlevel pair breaking, where an electron pair is broken up and one electron is transferred to another ℓ subsystem, become important.

At strong coupling, the electron pairs partially occupy about $\mu = 2G/\epsilon_1$ single-particle ℓ levels around the Fermi level L_F. All these μ single-particle levels become relevant in the pair-breaking process, raising the degeneracy of states due to pair breaking so that $J_{\rm 1bp}/J_{\rm gs} \approx 4C_2^{\mu(2L_F+1)} \approx 8L_F^2\mu^2$ for even bubbles and similarly $J_{\rm 1bp}/J_{\rm gs} \approx 8L_F^2\mu^2/3$ for odd bubbles.

D. Parity effect

From the preceding discussion, it is clear that there appears a parity effect. The presence of an unpaired electron in the odd bubbles alters the degeneracy ratio of the broken-pair state over the ground state. The presence of the unpaired electron also changes the pair-breaking energy to $\Delta_{L_F} = 2L_FG$ as compared with $\Delta_{L_F} = (2L_F+1)G$ for the even bubble. The estimate for the temperature T^* at which the broken-pair states start being populated will therefore also be different for even and odd cases. In particular, we have for the even case

$$k_BT^*_{\rm even} \approx \frac{(2L_F+1)G}{\ln(8L_F^2\mu^2)}, \tag{11}$$

with $\mu = \max[1, 2G/\epsilon_1]$, and for the odd case

$$k_BT^*_{\rm odd} \approx \frac{2L_FG}{\ln(8L_F^2\mu^2/3)}. \tag{12}$$

The location of these temperatures is indicated by arrows in Figs. 2 and 3. The estimates (11) and (12) are in good agreement with the temperatures at which $C(T)$ increases. Note that for even bubbles, the rise of the specific heat seems to show an initial "shoulder," and $T^*_{\rm even}$ is a bit smaller than $T^*_{\rm odd}$. This shoulder in the specific heat corresponds to the first pair-breaking transition. What makes it different from the following pair-breaking transitions? As implied from Fig. 1 depicting the density of states, the relative increase in D_δ due to the first pair-breaking transition is larger than that for further pair-breaking transitions. Moreover, the energy separation of states with one broken pair from adjacent states is larger than that of states with more than one broken pair.

From Eqs. (11) and (12), the relative difference between the characteristic temperature for odd and even bubbles is

$$(T^*_{\rm odd} - T^*_{\rm even})/T^*_{\rm even} = \left(\frac{\ln(3)}{\ln(8L_F^2\mu^2)} - \frac{1}{2L_F+1}\right) \times \left(1 - \frac{\ln(3)}{\ln(8L_F^2\mu^2)}\right)^{-1}. \quad (13)$$

For MEBs with large numbers of electrons ($N \gg 1$), the angular momentum L_F increases with N approximately as $\sqrt{N/2}$. With increasing N, also the parameter $\mu = 2G/\epsilon_1$ rises (it is about 11.6 for $N=10^3$ and 170 for $N=10^6$). Therefore, for sufficiently large N, inequalities $\ln(3) \ll \ln(8L_F^2\mu^2) \ll 2L_F+1$ are satisfied so that Eq. (13) takes the form

$$(T^*_{\rm odd} - T^*_{\rm even})/T^*_{\rm even} \approx \ln(3)/\ln(8L_F^2\mu^2). \quad (14)$$

The relative difference $(T^*_{\rm odd} - T^*_{\rm even})/T^*_{\rm even}$, described by Eq. (14), reflects the fact that—as discussed in the preceding section—for odd bubbles the ratio $J_{\rm 1bp}/J_{\rm gs}$ is approximately 3 times smaller as compared to that in even bubbles. With increasing N, the ratio $J_{\rm 1bp}/J_{\rm gs}$ strongly increases, while the relative difference in $J_{\rm 1bp}/J_{\rm gs}$ between odd and even bubbles remains the same at any $L_F \gg 1$. Since the characteristic temperature T^* depends on $J_{\rm 1bp}/J_{\rm gs}$ logarithmically [see Eq. (10)], the effect of the aforementioned difference in $J_{\rm 1bp}/J_{\rm gs}$ on $(T^*_{\rm odd} - T^*_{\rm even})/T_{\rm even}$ weakens with increasing N. As a result, the relative difference between the characteristic temperature for odd and even bubbles decreases with increasing N, but slowly. The characteristic temperature for multielectron bubbles with an even number of electrons, is shown in panel (a) of Fig. 4 as a function of the number of electrons in the bubble and the pressure exerted on the bubble. The pressure on a multielectron bubble increases the electron-ripplon coupling, and thus G, and T^*. The relative difference between the even and odd cases, as given by Eq. (13), is shown in panel (b). Even for fairly large numbers of electrons, $N \sim 10^6$, the $T^*_{\rm odd}$ is 4% higher than $T^*_{\rm even}$.

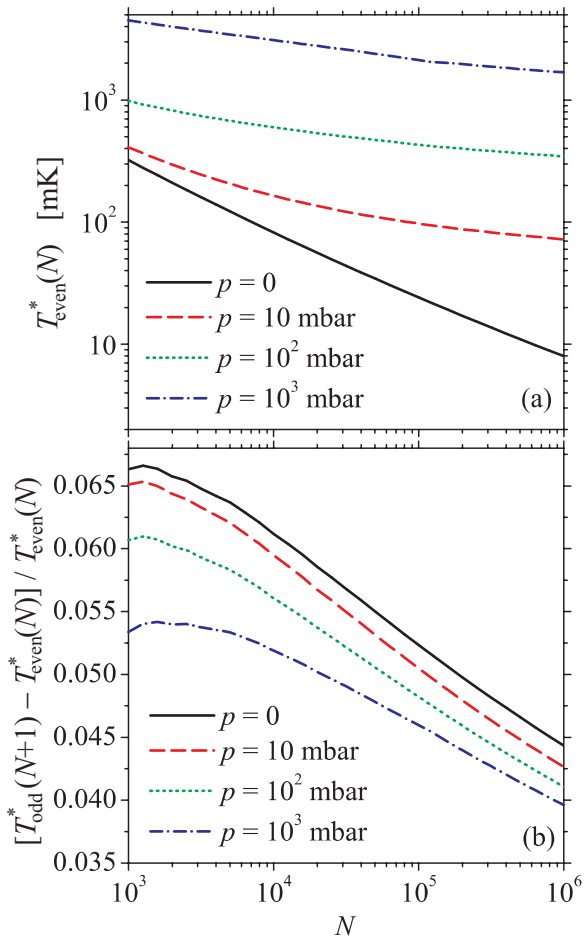

FIG. 4. (Color online) The characteristic temperature above which states with broken pairs become populated is shown as a function of the number of electrons on the sphere in panel (a) for an even number of electrons. In panel (b) the relative difference between the characteristic temperatures of even and odd systems is shown. Here p is the pressure on a multielectron bubble.

IV. CONCLUSIONS

In this paper, we have focused our discussion on the spherical electron system as it is realized in multielectron bubbles, even though the results presented here are more general, and valid for all the systems well described by the Hamiltonian (2). This BCS-type Hamiltonian on the sphere can be solved analytically using Richardson's method, and the specific heat is calculated from the energy level spectrum and the level degeneracies, or from the density of states. The ground state of the system is a state with strong BCS-type pair correlations. We show that the specific heat shows a sharp increase as soon as the temperature is large enough to populate the many-body states that contain broken pairs. The temperature at which the specific heat starts to increase constitutes a characteristic temperature T^* that separates the BCS-type pair-correlated state below T^* from the broken-pair states above T^*. This definition relates T^* to the critical temperature for the onset of superconductivity that can be derived from measuring the specific heat of a superconducting sample. It is important to note that the procedure followed here is not able to distinguish whether the BCS-tape pair-correlated state appears due to a phase transition or due to a smooth evolution from the "normal" Fermi liquid. The presence of an unpaired electron in spherical systems with an odd number of electrons significantly affects both the specific heat and T^*: we find that for multielectron bubbles with odd numbers of electrons T^* is roughly 4–6 % larger than in the even case. This persistent parity effect is present even for a large total number of electrons.

ACKNOWLEDGMENTS

The authors gratefully acknowledge stimulating discussions with V. M. Fomin. One of the authors (J.T.) is supported financially by the Fonds voor Wetenschappelijk Onderzoek-Vlaanderen. This research has been supported financially by the FWO-V Contracts Nos. G.0356.06, G.0115.06, G.0435.03, G.0306.00, the WOG Contract No. WO.025.99N, and the GOA BOF UA 2000 UA. Part of this work was also supported by the Department of Energy, Grant No. DE-FG02-ER45978. One of the authors (J.T.) gratefully acknowledges support of the Special Research Fund of the University of Antwerp, BOF NOI UA 2004.

*Current address: Department of Theoretical Physics, State University of Moldova, Str. A. Mateevici 60, MD-2009 Kishinev, Republic of Moldova.

[1] L. E. J. Brouwer, Math. Ann. **71**, 97 (1912).
[2] A. Goker and P. Nordlander, J. Phys.: Condens. Matter **16**, 8233 (2004); J. Tempere, I. F. Silvera, and J. T. Devreese, J. Low Temp. Phys. **138**, 457 (2005).
[3] M. Encinosa, Physica E (Amsterdam) **28**, 209 (2005); ,Phys. Rev. A **73**, 012102 (2006).
[4] R. D. Averitt, D. Sarkar, and N. J. Halas, Phys. Rev. Lett. **78**, 4217 (1997).
[5] C. Amovilli, I. A. Howard, D. J. Klein, and N. H. March, Phys. Rev. A **66**, 013210 (2002); N. Mizorogi, M. Kiuchi, K. Tanaka, R. Sekine, and J. Aihara, Chem. Phys. Lett. **378**, 598 (2003).
[6] A. P. Volodin, M. S. Khaikin, and V. S. Edelman, Pis'ma Zh. Eksp. Teor. Fiz. **26**, 707 (1977) [JETP Lett. **26**, 543 (1977)]; U. Albrecht and P. Leiderer, Europhys. Lett. **3**, 705 (1987).
[7] J. Tempere, I. F. Silvera, and J. T. Devreese, Phys. Rev. Lett. **87**, 275301 (2001).
[8] S. A. Jackson and P. M. Platzman, Phys. Rev. B **24**, 499 (1981); O. Hipólito, G. A. Farias, and N. Studart, Surf. Sci. **113**, 394 (1982).
[9] J. Tempere, V. N. Gladilin, I. F. Silvera, and J. T. Devreese, Phys. Rev. B **72**, 094506 (2005).
[10] C. T. Black, D. C. Ralph, and M. Tinkham, Phys. Rev. Lett. **76**, 688 (1996).
[11] J. von Delft, A. D. Zhaikin, D. S. Golubev, and W. Tichy, Phys. Rev. Lett. **77**, 3189 (1996).
[12] K. A. Matveev and A. I. Larkin, Phys. Rev. Lett. **78**, 3749 (1997).
[13] R. W. Richardson, Phys. Lett. **3**, 277 (1963).
[14] R. W. Richardson and N. Sherman, Nucl. Phys. **52**, 221 (1964).
[15] J. M. Román, G. Sierra, and J. Dukelsky, Phys. Rev. B **67**, 064510 (2003).
[16] A. Di Lorenzo, R. Fazio, F. W. J. Hekking, G. Falci, A. Mastellone, and G. Giaquinta, Phys. Rev. Lett. **84**, 550 (2000).
[17] J. Dukelsky, S. Pittel, and G. Sierra, Rev. Mod. Phys. **76**, 643 (2004).
[18] V. N. Gladilin, V. M. Fomin, and J. T. Devreese, Phys. Rev. B **70**, 144506 (2004).